# Dopamine increases protein synthesis in hippocampal neurons enabling dopamine-dependent LTP

Fuchsberger T[1*], Stockwell I[2], Woods M[1], Brzosko Z[1], Greger I[2], Paulsen O[1*]

[1]Department of Physiology, Development and Neuroscience, Physiological Laboratory, University of Cambridge, UK.

[2]Neurobiology Division, MRC Laboratory of Molecular Biology, Cambridge, UK.

*Corresponding authors: tf337@cam.ac.uk, op210@cam.ac.uk

Number of pages: 24

Number of figures: 4 main + 2 supplemental

Word count: Abstract,194; Main text, 4,072; Methods, 2,050

Number of references: 50

## Abstract

The reward and novelty related neuromodulator dopamine plays an important role in hippocampal long-term memory, which is thought to involve protein synthesis-dependent synaptic plasticity. However, the direct effects of dopamine on protein synthesis, and the functional implications of newly synthesized proteins for synaptic plasticity, have not yet been investigated. We have previously reported that timing-dependent synaptic depression (t-LTD) can be converted into potentiation by dopamine application during synaptic stimulation (Brzsoko et al., 2015) or postsynaptic burst activation (Fuchsberger et al., 2022). Here we show that dopamine increases protein synthesis in mouse hippocampal CA1 neurons, enabling dopamine-dependent long-term potentiation (DA-LTP). We found that neuronal activity is required for the dopamine-induced increase in protein synthesis, which is mediated via the $Ca^{2+}$-sensitive adenylate cyclase (AC) subtypes 1/8, cAMP, and cAMP-dependent protein kinase (PKA). Furthermore, dopamine induced a protein synthesis-dependent increase in the AMPA receptor subunit GluA1, but not GluA2. We found that DA-LTP is absent in GluA1 knock-out mice and that it requires calcium-permeable AMPA receptors. Taken together, our results suggest that dopamine together with neuronal activity controls synthesis of plasticity-related proteins, including GluA1, which enable DA-LTP via a signalling pathway distinct from that of conventional LTP.

## INTRODUCTION

An important role of dopamine in hippocampal long-term memory has long been recognised (O'Carroll et al., 2006; Rossato et al., 2009; Shohamy and Adcock., 2010; Takeuchi et al., 2016). Long-term memory is thought to be encoded by synaptic plasticity, in particular long-term potentiation (LTP; Bliss and Lømo, 1973) which, based on its duration, has been divided into an early phase and a protein synthesis-dependent late phase (Frey et al., 1988). Dopaminergic signalling has been implicated specifically in 'late-phase' LTP (Frey et al., 1990; Huang and Kandel, 1995; Matthies et al., 1997). Dopamine acts on G-protein-coupled receptors which activate adenylate cyclases (AC) to generate cAMP, which in turn activates several effectors, including the cAMP-dependent protein kinase (PKA). PKA has several downstream targets which ultimately regulate transcription (Sassone-Corsi, 1995; Kebabian and Calne, 1997; Mayr and Montminy, 2001). Although the requirement of dopamine for protein synthesis-dependent LTP has been well established, the underlying cellular mechanisms of how dopamine modulates activated synapses via protein synthesis-dependent mechanisms remains poorly understood.

In order to selectively label newly synthesized proteins, we used a puromycin-based assay for surface sensing of translation (SUnSET) (Schmidt et al., 2009) in acute mouse hippocampal slices. We found that dopamine increases protein synthesis in hippocampal neurons. We then investigated whether protein synthesis is required for a recently described dopamine-dependent form of plasticity (DA-LTP) which, although being rapid in onset, otherwise shares properties with 'late-phase' LTP (Brzosko et al., 2015; Fuchsberger et al., 2022). Whilst conventional 'early' LTP induced by a spike-timing-dependent plasticity protocol (t-LTP; Bi and Poo, 1998) was unaffected, DA-LTP was completely abolished by either of two different protein synthesis inhibitors.

A previous study in primary cultured hippocampal neurons reported that dopaminergic signalling increases the surface expression of the AMPA receptor subunit GluA1 (Smith et al., 2005), which has been widely studied in the context of LTP (Huganir and Nicoll, 2013; Diering and Huganir, 2018). Whereas most hippocampal AMPA receptors are heteromeric, incorporating the GluA2 subunit, making the receptor calcium-impermeable, GluA1 may form homomeric calcium-permeable AMPA receptors (CP-AMPARs) (Burnashev et al., 1992; Wenthold et al., 1996). As well as enabling calcium-permeability of the AMPAR, by lacking GluA2, the extracellular N-terminal domain of GluA1 homomers is highly flexible, which alters the gating of the receptor and hinders its synaptic anchoring (Zhang et al., 2023; Stockwell et al., 2024). CP-AMPARs have been implicated in some forms of LTP (Plant et al., 2006; Guire et al., 2008, Purkey et al., 2020), including a PKA-dependent form of plasticity (Park et al., 2021).

We found that levels of the GluA1 receptor subunit, but not GluA2, were upregulated in response to dopamine in a protein synthesis-dependent manner. Moreover, DA-LTP was absent in a GluA1 genetic knock-out mouse model, while conventional t-LTP remained intact. These findings suggest that newly synthesized GluA1 receptor subunits mediate the expression of DA-LTP, possibly by forming GluA1

homomeric CP-AMPARs. Indeed, while blocking CP-AMPARs did not interfere with conventional t-LTP, they were required for DA-LTP.

## RESULTS

### Dopamine increases protein synthesis in CA1, which is required for dopamine-dependent long-term potentiation (DA-LTP)

We hypothesized that application of dopamine induces synthesis of proteins that are required for the expression of DA-LTP. To address this, we first investigated whether dopamine directly affects the protein synthesis in hippocampal neurons. In order to exclusively visualise newly synthesized proteins in hippocampal slices we used a puromycin (PMY)-based SUnSET assay (Schmidt et al., 2009). Labelling was achieved by incubating acute hippocampal slices in artificial cerebrospinal fluid (aCSF) containing 3 µM PMY for 30 minutes (**Figure 1A**). As expected, slices incubated with PMY showed a significantly higher PMY intensity than those without (control, 0.39 ± 0.023, n = 9, vs +PMY, 0.54 ± 0.03, $t(16) = 3.98$, $p = 0.001$) (**Figure 1B and C**), confirming specificity of the antibody labelling approach. Furthermore, we tested whether PMY incorporation and labelling are specific to protein synthesis by adding the protein synthesis inhibitor cycloheximide (CHX) or anisomycin (AM) to the slices. We found that 30 minutes preincubation with CHX significantly reduced the PMY signal, confirming the specificity of the labelling approach (PMY, 1.8 ± 0.45, n = 7 vs PMY+CHX, 0.4 ± 0.05, n = 8, $t(6) = 3.1$, $p = 0.02$) (**Figure 1—figure supplement S1A and B**), as did 2 hr preincubation with AM (PMY, 0.6 ± 0.14, n = 4 vs PMY+AM, 0.16 ± 0.03, n = 5, $t(3.2) = 3.1$, $p = 0.048$) (**Figure 1—figure supplement S1C and D**).

Strikingly, when applying dopamine the PMY signal was significantly increased compared to slices without dopamine (PMY, 0.54 ± 0.03, n = 9 vs PMY+DA, 0.8 ± 0.02, n = 16, $p < 0.001$) (**Figure 1B and C**). We next examined the effect of the D1/D5 receptor agonist SKF38393, and found that it stimulates protein synthesis to a similar extent as dopamine, with no significant difference between those two conditions (PMY+DA, 0.8 ± 0.02, n = 16, vs PMY+SFK, 0.79 ± 0.026, n = 9, $p > 0.99$), and significantly different to PMY alone (PMY, 0.54 ± 0.03, n = 9 vs PMY+SFK, 0.79 ± 0.026, n = 9, $p < 0.001$) (**Figure 1B and C**). We next tested whether the dopamine-induced increase in protein synthesis could be prevented by application of D1/5 and D2 receptor antagonists. Using SCH23390, a selective antagonist at D1 (Ki = 0.2 nM) and D5 (Ki = 0.3 nM) receptor subtypes, and Sulpiride, a D2 antagonist (Ki = 8 nM), we found that the dopamine-induced increase in PMY signal was prevented (PMY+DA, 0.8 ± 0.019, n = 16, vs PMY+DA+SCH23390/Sulpiride, 0.61 ± 0.029, n = 8, $p < 0.001$; all p values reported above from post-hoc Tukey's HSD test, after confirming a statistically significant difference between at least two groups in one-way ANOVA; $F(4, 46) = 49.55$, $p < 0.001$) (**Figure 1B and C**).

To confirm the effect of dopamine on protein synthesis with an alternative quantification method, acute hippocampal slices were incubated as above and homogenates prepared for western blot analysis of the micro-dissected CA1 region. As expected, without PMY incubation the signal was virtually absent compared to samples with PMY (neg control, 5.44 ± 1.84, n = 5, vs +PMY, 97.24 ± 20.72, n = 5, p = 0.01). Dopamine

application significantly increased the PMY signal (PMY, 97.24 ± 20.72, n = 5, vs PMY+DA = 201.2 ± 25.3, n = 5, p = 0.006; p values reported from post-hoc Tukey's HSD test after one-way ANOVA; $F(3, 16) = 19.85$, $p < 0.0001$) (**Figure 1D and E**).

We then tested whether newly synthesized proteins are required for DA-LTP, which can be induced by a spike timing-dependent long-term depression (t-LTD) pairing protocol followed by dopamine application during low-frequency afferent stimulation, converting synaptic depression into potentiation (Brzosko et al., 2015). In contrast, conventional t-LTD, induced by a post-before-pre pairing without dopamine application leads to synaptic depression, whereas a pre-before-post t-LTP protocol induces synaptic potentiation (Bi and Poo, 1998; Feldman, 2012). We confirmed that application of dopamine after the pairing protocol (Δt = -20 ms) induces robust synaptic potentiation (145.4% ± 15.62% vs 100%, $t(9) = 2.9$, $p = 0.0173$, n = 10) (**Figure 1F and G**). Dopamine application alone had no effect on synapses that did not undergo prior pairing (107% ± 13.5% vs 100%, $t(9) = 0.54$, $p = 0.60$, n = 10) (**Figure 1—figure supplement S1E and G**). When delivering the protein synthesis inhibitor anisomycin (AM) to the postsynaptic cell through the recording pipette, DA-LTP was fully blocked, leaving synaptic depression instead (DA+AM, 56% ± 9% vs 100%, $t(5) = 4.8$, $p = 0.0047$, n = 6), which was significantly different from dopamine without AM (DA 145.4% ± 15.62% vs DA+AM 56% ± 9%, $t(14) = 4.129$, $p = 0.001$) (**Figure 1F and G**). To exclude the possibility that the effect of AM on blocking DA-LTP is mediated via other signalling pathways affected by AM (Croons et al., 2009; Hazzalin et al., 1998; Kyriakis et al., 1994) rather than by specific inhibition of protein synthesis, we used cycloheximide (CHX), an alternative blocker of protein synthesis. We found that loading CHX into the postsynaptic cell through the recording pipette also completely blocked DA-LTP, leaving synaptic depression instead (DA+CHX, 55% ± 12% vs 100%, $t(5) = 3.7$, $p = 0.0133$, n = 6) (**Figure 1F**), which was significantly different from dopamine without CHX (DA 145.4% ± 15.62% vs DA+CHX 55% ± 12%, $t(14) = 4.05$, $p = 0.001$) (**Figure 1F and G**). We also confirmed that postsynaptically applied AM or CHX had no effect on baseline synaptic transmission throughout the 60-minute duration of the experiment in the control pathway (no pairing +AM, 104 ± 17% vs 100%, $t(5) = 0.23$, $p = 0.83$, n = 6; and no pairing +CHX, 98 ± 6% vs 100%, $t(5) = 0.32$, $p = 0.76$, n = 6) (**Figure 1—figure supplement S1F and G**).

In contrast, when we used a t-LTP protocol (Δt = +10 ms) while CHX was loaded into the postsynaptic cell, we still observed robust potentiation (t-LTP + CHX, 158% ± 19% vs 100%, $t(5) = 3.11$, $p = 0.0265$, n = 6, **Figure 1H**), and, as expected, there was no significant effect of CHX on the control pathway (CHX, 87% ± 13% vs 100%, $t(5) = 0.97$, $p = 0.374$, n = 6, **Figure 1H**). These results demonstrate that DA-LTP, but not conventional t-LTP, requires postsynaptic protein synthesis, revealing two different signalling pathways for LTP, one of which requires dopamine and protein synthesis, while the other one does not.

**Dopamine and neuronal activity mediate increase in protein synthesis**

DA-LTP requires neuronal activation during dopamine application either via subthreshold synaptic stimulation (Brzosko et al., 2015) or postsynaptic bursts (Fuchsberger et al., 2022). Thus, we investigated whether neuronal activity is also required for the dopamine-induced increase in protein synthesis.

To test this, acute hippocampal slices were treated with tetrodotoxin (TTX), a voltage-gated sodium channel blocker, during PMY incubations (**Figure 2A**). We confirmed using whole-cell patch clamp recordings that application of TTX inhibits spontaneous EPSPs in CA1 pyramidal neurons in our preparations (**Figure 2B**). Using the PMY labelling assay, we found that TTX incubation alone did not significantly alter PMY labelling, suggesting that the baseline level of protein synthesis is not affected by blocking neuronal activity for 30 minutes (control, 0.55 ± 0.033, n = 8, vs TTX, 0.53 ± 0.026, n = 8, p = 0.90) (**Figure 2A and C**). However, TTX significantly diminished the dopamine-induced increase in protein synthesis (DA, 0.83 ± 0.024, n = 9, vs DA+TTX, 0.65 ± 0.017, n = 9, p < 0.001). Nevertheless, the dopamine-induced increase in protein synthesis was not fully blocked by TTX, as it remained significantly higher in the presence of dopamine and TTX compared to TTX alone (TTX+DA, 0.65 ± 0.017, n = 9, vs TTX 0.53 ± 0.026, n = 8, p = 0.005; p values reported from post-hoc Tukey's HSD test after one-way ANOVA; F (3, 30) = 30.57, p < 0.001) (**Figure 2A and C**).

**Dopamine-induced increase in protein synthesis is mediated via AC1/8 and PKA**

We then sought to identify the signalling pathway that mediates the changes in protein synthesis in response to dopamine and neuronal activity. D1 and D5 dopamine receptors are known to activate adenylate cyclases (AC), which increase cyclic adenosine monophosphate (cAMP) activating the cAMP-dependent protein kinase (PKA) (Sassone-Corsi, 2012). We used the PMY incubation assay to assess the protein synthesis in the presence of Rp-cAMPS, a cell-permeable cAMP analogue which acts as an inhibitor of PKA. We found that application of Rp-cAMPS had no significant effect on protein synthesis in control conditions (control, 1.16 ± 0.10, n = 10, vs Rp-cAMPS 1.74 ± 0.35, n = 8, p = 0.25), but completely blocked the dopamine-induced increase in PMY levels (DA, 2.16 ± 0.23, n = 10, vs DA+Rp-cAMPS, 1.30 ± 0.12, n = 9, p = 0.029; p values reported from post-hoc Tukey's HSD test after one-way ANOVA; F (3, 33) = 4.912, p = 0.0062) (**Figure 2D and E**).

AC subtypes 1 and 8 are additionally activated by $Ca^{2+}$, which would make them attractive candidates to mediate activity-dependent dopamine signalling. We therefore tested whether DA-LTP requires these adenylate cyclases using an AC1/AC8 double knock-out (DKO) mouse model (Wang et al., 2003). We found that DA-LTP was completely absent in AC1/AC8 DKO mice, leaving synaptic depression instead (AC DKO 74.4% ± 10.3% vs 100%, t(6) = 2.6, p = 0.041, n = 7), which was significantly different to DA-LTP in WT mice (WT 125.1% ± 15.8%, n = 6, vs AC DKO 74.4% ± 10.3%, n = 7, t(11) = 4.2, p = 0.0016) (**Figure 2F and H**). To test whether PKA signalling is required for DA-LTP, we loaded the PKA blocker, protein kinase inhibitor-(6-22)-amide (PKI), into the postsynaptic cell through the recording pipette. Dopamine application after the t-LTD priming protocol followed by subthreshold synaptic stimulation failed to convert depression into potentiation in the presence of PKI (DA+PKI 81% ± 3% vs 100%, t(5) = 6.1, p = 0.0017, n = 6), which was significantly different to the effect of dopamine application without PKI (DA+PKI 81% ± 3.1% vs DA 125.1% ± 15.8%, t(10) = 6.2, p = 0.0001) (**Figure 2G and H**).

**Dopamine increases GluA1, which is required for DA-LTP**

It has been reported in hippocampal primary neuronal culture that dopaminergic stimulation enhances surface expression of the AMPA receptor subunit GluA1 (Smith et al., 2005). To confirm whether this finding holds in an acute slice preparation, we tested the effect of dopamine on GluA1 levels in the micro-dissected CA1 region. Using western blot analysis, we found that dopamine application induces a significant increase in the GluA1 receptor subunit compared to control conditions (control, 0.44 ± 0.071, n = 7, vs DA, 1.03 ± 0.18, n = 7, t(6) = 3.27, p = 0.02) (**Figure 3A and B**). Importantly, when we blocked protein synthesis with cycloheximide, the GluA1 increase was prevented (DA, 1.03 ± 0.18, n = 7, vs DA+CHX, 0.74 ± 0.15, n = 7, t(6) = 3.33, p = 0.02) (**Figure 3A and B**) showing that the dopamine-induced increase in GluA1 is protein synthesis-dependent. In contrast, when we measured the levels of the GluA2 subunit under the same conditions, we could not detect significant differences between dopamine-treated and control CA1 (control, 0.67 ± 0.17, n = 5, vs DA, 0.61 ± 0.15, n = 5, t(4) = 0.69, p = 0.53) (**Figure 3C and D**), nor in the presence of CHX (DA 0.61 ± 0.15, n = 5, vs DA+CHX, 0.60 ± 0.15, n = 5, t(4) = 0.75, p = 0.5) (**Figure 3C and D**).

We next investigated the functional implications of GluA1 for DA-LTP using a GluA1 knock-out (KO) mouse model. GluA1 plays an important role in synaptic plasticity (Zamanillo et al., 1999;Granger et al., 2013; Park et al., 2019, Purkey et al*.,* 2020), but is not required for all forms of LTP (Hoffman et al., 2002; Romberg et al., 2009; Frey et al., 2009). Thus, we first tested whether we could induce conventional t-LTP and t-LTD in slices of GluA1 KO mice. We found that a t-LTP protocol (Δt = +10 ms) led to synaptic potentiation, albeit of somewhat reduced magnitude (t-LTP GluA1 KO, 125% ± 9.4% vs 100%, t(5) = 2.6, p = 0.046, n = 6) (**Figure 3E and G**), while a t-LTD protocol (Δt = -20 ms) induced synaptic depression (t-LTD GluA1 KO, 65.9% ± 8.8% vs 100%, t(12) = 3.9, p = 0.002, n = 13) (**Figure 3E and G**). Strikingly, however, in the GluA1 KO mice, application of dopamine failed to convert t-LTD into LTP (DA-LTP GluA1 KO, 90% ± 7.2%, n = 8; **Figure 3F**) and the resulting depression was not significantly different from t-LTD without dopamine (t-LTD vs DA-LTP, t(19) = 1.905, p = 0.07) (**Figure 3G**). Taken together, these results suggest that newly synthesized GluA1 subunits are required for expression of DA-LTP.

**DA-LTP requires CP-AMPARs**

GluA1 homomers may form CP-AMPARs in the hippocampus (Wenthold et al., 1996). A transient increase in CP-AMPARs has been reported in some forms of LTP (Plant et al., 2006; Guire et al., 2008; Park et al., 2019; Purkey et al*.,* 2020), including a PKA-dependent form of plasticity (Park et al., 2021). Since we observed a protein synthesis-dependent increase in the GluA1, but not GluA2, AMPA receptor subunit after dopamine application, we hypothesised that CP-AMPA receptors might be involved in DA-LTP.

We compared the effect of NASPM, a selective CP-AMPAR antagonist, on conventional t-LTP (Δt = +10 ms) to the effect of NASPM on DA-LTP. We found that robust t-LTP was elicited in the presence of extracellular NASPM (139.6% ± 10.9% vs 100%, t(5) = 3.6, p = 0.015, n = 6) (**Figure 4A and C**). In contrast, when applying NASPM during a DA-LTP protocol, potentiation was completely prevented (74.86% ± 15.18 vs 100%, t(5) = 1.66, p = 0.16, n = 6) (**Figure 4B and C**). This shows that CP-AMPARs are indeed required for DA-LTP. The selective increase of GluA1 receptor subunit levels seen in response to dopamine (**Figure 3A-D**) suggests that CP-AMPARs are required for expression of DA-LTP.

We have recently reported that, in addition to synaptic activation, postsynaptic burst stimulation can also induce DA-LTP, which is mediated via the same AC-PKA signalling pathway and also requires protein synthesis (Fuchsberger et al., 2022). Synaptically induced DA-LTP develops gradually, while burst-induced DA-LTP shows rapid potentiation. We therefore used burst-induced DA-LTP to test whether a transient increase in CP-AMPARs may be required for potentiation. We applied NASPM during or shortly after the plasticity protocol to test whether this affects the expression of DA-LTP. We found that application of NASPM during burst stimulation completely prevented synaptic potentiation (78.17% ± 10.87% vs 100%, $t(6) = 2.01$, $p = 0.091$, $n = 7$) (**Figure 4D and F**). However, when applying NASPM 7 minutes *after* burst stimulation, we observed an initial potentiation (117.6% ± 3.88% vs 100%, $t(6) = 4.52$, $p = 0.0063$, $n = 6$), which gradually returned to baseline in the presence of NASPM (91.1% ± 10.9% vs 100%, $t(5) = 0.815$, $p = 0.45$, $n = 6$) (**Figure 4E and F**).

To confirm these results with an alternative CP-AMPAR blocker we applied IEM1460 extracellularly. Conventional t-LTP ($\Delta t = +10$ ms) was compared to DA-LTP in the presence of IEM1460 throughout the recording, which were significantly different (t-LTP+IEM1460, 142.0% ± 20.93%, $n = 7$, vs DA-LTP+IEM1460, 80.3% ± 8.1%, $n = 7$, $t(12) = 2.75$, $p = 0.02$) (**Figure 4—figure supplement S4A, B and D**). When applied immediately *after* the pairing protocol, IEM1460 still prevented DA-LTP and left a synaptic depression instead (DA-LTP+IEM after, 67.5% ± 12.11% vs 100%, $t(8) = 2.68$, $p = 0.028$, $n = 9$) (**Figure 4—figure supplement S4C and D**). Taken together, these results suggest that DA-LTP, but not conventional t-LTP, requires CP-AMPARs for expression of synaptic potentiation.

## DISCUSSION

In summary, we investigated the effect of dopamine on protein synthesis in hippocampal neurons and how protein synthesis enables dopamine-dependent long-term potentiation (DA-LTP). We report four main findings: (1) Dopamine increases protein synthesis in an activity-dependent manner through the activation of PKA. (2) Dopamine enables a rapid onset protein synthesis-dependent form of synaptic potentiation (DA-LTP). (3) Dopamine increases the level of GluA1 but not GluA2 subunit of AMPA receptors. (4) Expression of DA-LTP requires GluA1 AMPA receptor subunit and $Ca^{2+}$-permeable (CP)-AMPARs, whereas t-LTP does not, suggesting the existence of two distinct forms of LTP.

Recent developments of protein synthesis labelling techniques enabled us to directly monitor protein synthesis in neurons in response to dopamine. We report that dopamine increases protein synthesis in pyramidal neurons in CA1 of acute hippocampal slices within minutes. This is consistent with previous reports from hippocampal and cortical neuronal cell culture systems, which showed that dopamine receptor agonist SKF-38393 enhances protein synthesis (Smith et al., 2005; David et al., 2020). We found that the dopamine-induced increase in protein synthesis is mediated by D1/D5 receptors via the AC-cAMP-PKA pathway (Mayr et al., 2001; Sassone-Corsi, 1995), which is also consistent with previously reported hippocampal cell culture results which showed that application of Sp-cAMPS, an activator of PKA, was

sufficient to induce an increase in protein synthesis (Smith et al., 2005). In addition, the AC-cAMP-PKA pathway induced by dopamine may affect several downstream targets and interact with other signalling pathways that could enhance protein synthesis. It has been reported in cortical primary neuronal cultures that D1, but not D2 receptors, increase protein synthesis via the mTOR-ERK pathway resulting in dephosphorylation of eEF2 (David et al., 2020).

Consistent with our previous results that burst-induced potentiation in the presence of dopamine requires postsynaptic PKA and protein synthesis (Fuchsberger et al., 2022), we found here that synaptic potentiation induced by low frequency synaptic stimulation in the presence of dopamine following a priming protocol, which would otherwise induce synaptic depression (Brzosko et al., 2015), also requires postsynaptic PKA and new protein synthesis. While conventional t-LTP remained intact, blocking protein synthesis in the postsynaptic neurons completely prevented DA-LTP, suggesting that dopamine induces the synthesis of plasticity-related proteins required for converting synaptic depression into potentiation.

DA-LTP shares properties with 'late-phase' LTP (L-LTP), which also requires dopamine signalling (Frey et al., 1990), PKA (Frey et al., 1993) and protein synthesis (Frey et al., 1988), and it was reported that protein synthesis was required hours after LTP induction for the maintenance of synaptic strength (Frey et al., 1988). In contrast, for the form of dopamine-dependent LTP studied here, protein synthesis was required ahead of or within the first few minutes of the induction protocol. Moreover, while previous studies have used extracellular application of protein synthesis inhibitors, here we specifically loaded the protein synthesis inhibitors into the postsynaptic neuron via the patch pipette, suggesting it is specifically postsynaptic protein synthesis that is required for DA-LTP.

We found that neuronal activity was also required for dopamine to increase protein synthesis, and we identified the $Ca^{2+}$-dependent AC subtypes AC1/AC8 as coincidence detector for the two signals, Gs-coupled dopamine D1/D5 receptor activation and $Ca^{2+}$ influx. Our results show that the AC1/AC8 subtypes and PKA are required for DA-LTP. These results suggest that dopamine application during neuronal activity induces the synthesis of plasticity-related proteins that enable synaptic potentiation.

Western blots showed that dopamine increased the levels of the AMPA receptor GluA1 subunit in a protein synthesis-dependent manner, but that the GluA2 subunit remained unchanged. This is consistent with a previous study in primary hippocampal cultured neurons which reported that dopaminergic signalling increases the surface expression of AMPA receptor subunit GluA1 (Smith et al., 2005). The selective increase of the GluA1 over GluA2 subunit is interesting because of the important role ascribed to the GluA1 subunit in LTP (Huganir and Nicoll, 2013; Diering and Huganir, 2018).

We report here that although conventional t-LTP could still be induced in a GluA1 KO mouse model, GluA1 was required for DA-LTP. These observations revealed a possible mechanism through which dopamine can modulate synaptic strength. Furthermore, the findings indicated another intriguing possibility, namely that GluA1 homomeric AMPA receptors, which are calcium-permeable, mediate the expression of DA-LTP. CP-

AMPA receptors appear to be required for some forms of LTP (Plant et al., 2006; Guire et al., 2008; Frey et al., 2009), while other studies found no involvement (Adesnik and Nicoll, 2007; Gray et al., 2007). Their role in synaptic plasticity remains controversial. We report here that they are required for DA-LTP, but not for conventional t-LTP. Importantly, even blocking CP-AMPARs after the pairing paradigm reversed DA-LTP, which strongly supports the possibility that they are required for expression of DA-LTP. Whether they also contribute to the induction of the dopamine-dependent potentiation induced by low-frequency afferent stimulation following a t-LTD priming protocol (Brzosko et al., 2015) remains unresolved.

In summary, our findings suggest a possible mechanism for how the reward-related neuromodulator dopamine may contribute to protein synthesis-dependent synaptic plasticity facilitating hippocampal long-term memory. However, understanding the signalling mechanisms underlying dopaminergic control of protein synthesis and synaptic weights is not only important for studying learning and memory mechanisms, but may also be important for pathophysiological processes. Dysregulation in dopamine systems has been long been implicated in drug addiction (for review see Dalley and Everitt, 2009), schizophrenia (for review see Kahn et al., 2015) as well as neurodegenerative diseases such as Parkinson's disease (for review see Poewe et al., 2017), and, more recently, also Alzheimer's disease (Nobili et al., 2017). Understanding signalling pathways underlying dopamine-dependent synaptic plasticity may help guide future research into alternative treatment options.

## METHODS

### Animals

Mice used for this study were housed at the Combined Animal Facility, Cambridge University. They were held on a 12-hr light/dark cycle at 19–23 °C and were provided with water and food ad libitum. Experiments were carried out using wildtype C57BL/6 J mice (Charles River Laboratories, UK), and the transgenic mouse lines adenylate cyclase (AC) subtypes 1 and 8 double knockout (AC1/AC8 DKO) mice and GluA1 knockout mice (GluA1 KO). The AC1/AC8 DKO mice have the genes for both AC1 and AC8 deleted globally. The mouse line was generated as described previously (Wang, et al., 2003) and was imported from Michigan State University, MI, US. The GluA1 KO mouse line was generated as described previously (Zamanillo et al., 1999) and was imported from the MRC Laboratory of Molecular Biology, Cambridge, UK.
All procedures were performed in accordance with the animal care guidelines of the UK Home Office regulations of the UK Animals (Scientific Procedures) Act 1986, and Amendment Regulations 2012, following ethical review by the University of Cambridge Animal Welfare and Ethical Review Body (AWERB). Animal procedures were authorized under Personal and Project licences held by the authors.

### Preparation of acute hippocampal slices

Male and female mice at postnatal days 12-19 were briefly anaesthetised with isoflurane (4% isoflurane in oxygen) and decapitated. The brain was rapidly removed into ice-cold artificial cerebrospinal fluid (aCSF)

(10 mM glucose, 26.4 mM $NaH_2CO_3$, 126 mM NaCl, 1.25 mM $NaH_2PO_4$, 3 mM KCl, 2 mM $MgSO_4$, 2 mM $CaCl_2$) bubbled with carbogen gas (95% $O_2$/5% $CO_2$) (pH 7.2, 270–290 mOsm/L) and glued to a vibrating microtome stage. Horizontal slices (350 µm) were sectioned with a vibratome (Leica VT 1200S, Leica Biosystems, Wetzlar, Germany) and were subsequently submerged in aCSF for at least 1 hr at room temperature (RT) in a storage chamber. Slices were used 1–6 hr after preparation.

## Electrophysiology

### Whole-cell recordings and synaptic plasticity

Individual slices were transferred to a submersion-type chamber for recordings, and superfused with aCSF (2 ml/min) at RT (24–26 °C). Neurons were visualized with an infrared differential interference contrast (DIC) microscope using a 40x water-immersion objective. Hippocampal subfields were identified and whole-cell patch-clamp recordings were performed on CA1 pyramidal neurons. Monopolar stimulation electrodes were placed in stratum radiatum for stimulation of Schaffer collaterals. Electrodes for test and control pathways were placed at the same distance (>100 µm) from either side of the recorded neuron. Patch pipettes (pipette resistance 4–7 MΩ) were pulled from borosilicate glass capillaries (0.68 mm inner diameter, 1.2 mm outer diameter) using a P-97 Flaming/Brown micropipette puller (Sutter Instruments Co., Novato, California, USA). Pipettes were filled with intracellular solution containing: 110 mM potassium gluconate, 4 mM NaCl, 40 mM HEPES, 2 mM ATP-Mg, 0.3 mM GTP (pH 7.2–7.3, 270–285 mOsm/L). The liquid junction potential was not corrected.

All experiments were performed in current-clamp mode. Cells were accepted for the experiment if their resting membrane potential was between −55 and −70 mV. Throughout the recording the membrane potential was held at −70 mV by direct current application via the recording electrode. All cells were tested for regular spiking responses to positive current steps (20 pA, 800 ms) characteristic of pyramidal neurons before the start of each recording.

TTX experiments were performed measuring spontaneous EPSPs for 5 minutes before and after adding 1 µM TTX to superfusing aCSF for 15 minutes.

Plasticity recordings were carried out as described previously (Brzosko et al., 2015). Briefly, excitatory postsynaptic potentials (EPSPs) were evoked alternately in two input pathways (test and control) by direct current pulses at 0.2 Hz (stimulus duration 50 µs) through metal stimulation electrodes. The stimulation intensity was adjusted (100 µA – 500 µA) to evoke an EPSP with peak amplitude between 3 and 8 mV. After a stable EPSP baseline period of at least 10 minutes, spike-timing-dependent plasticity (STDP) was induced in the test pathway by repeated pairings (100 times at 0.2 Hz) of single evoked EPSPs and single postsynaptic action potentials elicited with the minimum somatic current pulse (1 – 1.8 nA, 3 ms) via the recording electrode. Spike-timing intervals (Δt in ms) were measured between the onset of the EPSP and the onset of the action potential. Alternate stimulation of test and control EPSPs was resumed immediately after the pairing protocol and monitored for at least 40 minutes, except when the burst stimulation protocol was used for plasticity induction. In that case, stimulation of EPSPs was not resumed for an additional 10

minutes in the test pathway, and at the end of that period, five bursts, each of five action potentials at 50 Hz, were elicited with an inter-burst interval of 0.1 Hz by somatic current pulses (1.8 nA, 10 ms) via the recording electrode. Immediately after the bursts, stimulation of EPSPs was resumed and monitored for at least 30 minutes. Presynaptic stimulation frequency to evoke EPSPs remained constant throughout the experiment. The unpaired control pathway served as a stability control.

**Drug application**

Drugs were bath-applied to the whole slice through the perfusion system by dilution of concentrated stock solutions in aCSF, or by adding the drugs to the patch pipette solution when it was applied intracellularly to the postsynaptic cell only. For each set of recordings, interleaved control and drug conditions were carried out and were pseudo-randomly chosen. The following drugs were used in this study: 100 µM dopamine hydrochloride (Sigma–Aldrich, Dorset, United Kingdom), 10 µM cycloheximide (Tocris Bioscience), 0.5 mM anisomycin (stock solution in EtOH; Tocris Bioscience), 1 µM PKA inhibitor fragment (6-22) amide (Tocris Bioscience), 100 µM 1-naphthyl acetyl spermine trihydrochloride (NASPM trihydrochloride; Tocris Bioscience), 10 µM N,N,H,-trimethyl-5-[(tricyclo[3.3.1.13,7]dec-1-ylmethyl)amino]-1-pentanaminiumbromide hydrobromide (IEM1460; Tocris Bioscience).

**Data acquisition and data analysis of slice recordings**

Data were collected using an Axon Multiclamp 700B amplifier (Molecular Devices, Sunnyvale, California, USA). Data were filtered at 2 kHz and were acquired and digitized at 5 kHz using an Instrutech ITC-18 A/D interface board (Instrutech, Port Washington, New York, USA) and custom-made acquisition procedures in Igor Pro (WaveMetrics, Lake Oswego, Oregon, USA).

All experiments were carried out in current clamp mode, and only cells with an initial series resistance between 9 – 16 MΩ were included. Series resistance was compensated for by adjusting the bridge balance, and recordings were discarded if series resistance changed by more than 30%. Offline analyses of plasticity recordings were done using custom-made procedures in Igor Pro. EPSP slopes were measured on the rising phase of the EPSP as a linear fit between the time points corresponding to 25–30% and 70–75% of the peak amplitude.

For quantifications, the mean EPSP slope per minute of the recording was calculated from 12 consecutive sweeps and normalised to the baseline (each data point in source data files is the mean of 12 averaged EPSPs). Normalised EPSP slopes from the last 5 minutes of the baseline (immediately before pairing) and from the last 5 minutes of the recording were averaged. The magnitude of plasticity, as an indicator of change in synaptic weights, was defined as the average EPSP slope 40 minutes after the plasticity protocol expressed as a percentage of the average EPSP slope during baseline. In case of the burst-induction protocol, the change in synaptic weights, was defined as the average EPSP slope 30 minutes after the plasticity protocol expressed as a percentage of the average EPSP slope during baseline.

**Statistical analysis of slice recordings**

Statistical comparisons were performed using one-sample two-tailed, paired two-tailed, or unpaired two-tailed Student's *t*-test, with a significance level of $\alpha = 0.05$. Data are presented as mean ± SEM. Significance levels are indicated by $^{*}p < 0.05$, $^{**}p < 0.01$, $^{***}p < 0.001$.

**Protein synthesis labelling in acute hippocampal slices**

Incubation chambers were set up to submerge slices in oxygenated (95% $O_2$, 5% $CO_2$) aCSF containing a selection from the following drugs: 3 µM puromycin dihydrochloride (Sigma P8833), 100 µM dopamine hydrochloride (Sigma H8502), 10 µM SKF38393 (Sigma D047), 10 µM SCH23390 hydrochloride (Sigma D054), 50 µM sulpiride (Sigma S8010), 1 µM TTX (Tocris Bioscience), 10 µM cycloheximide (Tocris Bioscience), 0.5 mM anisomycin (stock solution in EtOH; Tocris Bioscience), 30 µM Rp-cAMPS (Tocris Bioscience).

Protein synthesis was measured using a puromycin labelling assay, based on the SUnSET method, as described previously (Schmidt et al., 2009). Briefly, 3 µM puromycin was used to incorporate into proteins during the elongation phase of synthesis (Figure 1A). After exactly 30 minutes of incubation with puromycin, samples were washed in phosphate-buffered saline (PBS), and further processed for immunohistochemistry or western blotting as described below. The specificity of the conjugated puromycin monoclonal antibody was confirmed with incubations of no-puromycin controls and protein synthesis inhibitors.

**Immunohistochemistry**

Immediately after incubations with puromycin slices were washed in PBS and fixed in 4% paraformaldehyde (PFA) in 1x PBS for 24 hr at 4 °C. Slices were subsequently washed 3 x 5 minutes in PBST 0.01% (DPBS ThermoFisher, Tween P1379 Sigma), permeabilised for 15 minutes in PBST 0.5% and washed in PBST 0.01% a further three times. Slices were incubated for 2 hr at room temperature in a blocking solution of 5% goat serum in PBST 0.0.1% (SigmaAldrich G9023) followed by an incubation overnight at 4 °C in blocking solution with anti-puromycin antibody (clone 12D10, MABE343; 1:500) AlexaFluor 488 or AlexaFluor 647 (MABE343-AF488 or MABE343-AF647; Merck). On the following day, slices were left on a shaker for 2 hr at RT, followed by 3 x 5 minutes washes in PBST 0.01%. Finally, slices were mounted onto microscope slides (ThermoScientific J1810AMNZ), allowed to dry for at least 2 hr at RT, then covered with Fluoroshield with Dapi mounting medium for nuclear staining (Sigma F6057) and sealed with coverslip sealant (Biotium 23005).

**Imaging and image analysis**

Immunohistochemical preparations were visualised using a confocal laser-scanning microscope (Leica TCS SP8). Z-stacks of hippocampal CA1 region were taken using an HC PL APO 20x/0.75 CS2 objective using the same exposure settings for all conditions that were compared to each other. AlexaFluor 647 was excited at 638 nm and emission detected at 671 nm; AlexaFluor488 was excited at 495 nm and emission detected at 519 nm, Dapi was excited at 359 nm, emission detected at 461 nm. Images were analysed using ImageJ.

To obtain normalised integrated density, the maximum intensity Z-projection of slices were extracted, from which the integrated density was measured and normalised to the corresponding nuclear staining (Dapi) Z-projection measurement. Normalised integrated density was plotted and statistical analysis was performed using one-way ANOVA and post-hoc Tukey's HSD test, following adherence to tests for normality and equality of variance. Significance level used was $\alpha = 0.05$ and indicated as $*p < 0.05$, $**p < 0.01$, $***p < 0.001$.

**Western blot analysis**

Acute hippocampal slices were prepared and incubated with various compounds as described above. After 30 minutes incubation, slices were rapidly dissected in aCSF to obtain the CA1 region, which were pooled for slices from each condition and flash frozen in liquid N2. Protein extraction buffer (150 mM NaCl, 1% Triton x-100, 50 mM TrisHCl pH 7.4 with protease inhibitor (11836170001 Roche)), at a volume adjusted to the tissue weight for each sample, was added to lyse the tissue for 1 hr at 4°C with frequent vortexing. Samples were centrifuged at 16,000 x g for 30 minutes at 4 °C and the supernatant was retained. Lysate was mixed with LDS sample buffer (Invitrogen NP0007) and boiled at 95 °C for 5 min, after which it was loaded onto a polyacrylamide gel (Bolt 4-12% Bis-Tris NW04127BOX). Loading was adjusted to achieve comparable actin signal. Proteins were transferred onto a nitrocellulose membrane using Trans-Blot Turbo Transfer (BioRad 1704158) and membranes were then blocked for 30 minutes at room temperature with 5% milk in TBST. Membranes were incubated with primary antibodies (anti-actin MAB1501R, anti-puromycin MABE343, anti-GluA1 AB1504, anti-GluA2 AF1050), washed 3 times in TBST, incubated with horseradish peroxidase (HRP)-coupled secondary antibody (Sigma) and washed a further 3 times. Membranes were developed using enhanced chemiluminescence and imaged with a ChemiDoc MP Imaging System (Biorad). Quantification of antibody staining was made using ImageJ. Integrated density of GluA1/2 bands was normalised to integrated density of actin in the corresponding lane. Statistical analysis was performed using one-way ANOVA and post-hoc Tukey's HSD test, following adherence to tests for normality and equality of variance. Significance level used was $\alpha = 0.05$ and indicated as $*p < 0.05$, $**p < 0.01$, $***p < 0.001$.

**References**


Adesnik H and Nicoll RA (2007) Conservation of glutamate receptor 2-containing AMPA receptors during long-term potentiation. *J. Neurosci*. **27**:4598–4602.

Bi GQ and Poo MM (1998) Synaptic modifications in cultured hippocampal neurons: dependence on spike timing, synaptic strength, and postsynaptic cell type. *J Neurosci.* **18**:10464-72.

Bliss TV and Lomo T (1973) Long-lasting potentiation of synaptic transmission in the dentate area of the anaesthetized rabbit following stimulation of the perforant path. *J Physiol.* **232**:331–56.

Brzosko Z, Schultz W, Paulsen O (2015) Retroactive modulation of spike timing-dependent plasticity by dopamine. *Elife* **4**:e09685.

Burnashev N, Monyer H, Seeburg PH, Sakmann B (1992) Divalent ion permeability of AMPA receptor channels is dominated by the edited form of a single subunit. *Neuron* **8**:189-98.

Coombs I, Bats C, Sexton CA, Studniarczyk D, Cull-Candy SG, Farrant M (2023) Enhanced functional detection of synaptic calcium-permeable AMPA receptors using intracellular NASPM. *Elife* **12**:e66765.

Croons V, Martinet W, Herman AG, Timmermans JP, De Meyer GR (2009) The protein synthesis inhibitor anisomycin induces macrophage apoptosis in rabbit atherosclerotic plaques through p38 mitogen-activated protein kinase. *J.Pharmacol.Exp.Ther*. **329**:856–64.

Diering GH, Huganir RL (2018) The AMPA Receptor Code of Synaptic Plasticity. *Neuron* **100**:314–329.

Dalley JW and Everitt BJ (2009) Dopamine receptors in the learning, memory and drug reward circuitry. Semin Cell Dev Biol. 20:403–410.

David O, Barrera I, Gould N, Gal-Ben-Ari S, Rosenblum K (2020) D1 dopamine receptor activation induces neuronal eEF2 pathway-dependent protein synthesis. *Front Mol Neurosci.* **13**:67.

Feldman DE. The spike-timing dependence of plasticity (2012*) Neuron* **75**: 556-571.

Frey MC, Sprengel R, Nevian T (2009) Activity pattern-dependent long-term potentiation in neocortex and hippocampus of GluA1 (GluR-A) subunit-deficient mice. *J Neurosci*. **29**:5587–5596.

Frey U, Krug M, Reymann KG, Matthies H (1988) Anisomycin, an inhibitor of protein synthesis, blocks late phases of LTP phenomena in the hippocampal CA1 region in vitro. *Brain Res*. **452**:57–65.

Frey U, Huang YY, Kandel ER (1993) Effects of cAMP simulate a late stage of LTP in hippocampal CA1 neurons. *Science* **260**:1661-1664.

Frey U, Schroeder H, Matthies H (1990) Dopaminergic antagonists prevent long-term maintenance of posttetanic LTP in the CA1 region of rat hippocampal slices. *Brain Research* **522**:69–75.

Fuchsberger T, Clopath C, Jarzebowski P, Brzosko Z, Wang H, Paulsen O (2022) Postsynaptic burst reactivation of hippocampal neurons enables associative plasticity of temporally discontiguous inputs. *Elife* **11**:e81071.

Granger AJ, Shi Y, Lu W, Cerpas M, Nicoll RA (2013) LTP requires a reserve pool of glutamate receptors independent of subunit type. *Nature* **493**: 495–500.

Gray EE, Fink AE, Sarinaña J, Vissel B, O'Dell TJ (2007) Long-term potentiation in the hippocampal CA1 region does not require insertion and activation of GluR2-lacking AMPA receptors. *J. Neurophysiol*. **98**: 2488–2492.

Guire ES, Oh MC, Soderling TR, Derkach VA (2008) Recruitment of calcium-permeable AMPA receptors during synaptic potentiation is regulated by CaM-kinase I. *J Neurosci*. **28**:6000–6009.

Hazzalin CA, Le Panse R, Cano E, Mahadevan LC (1998) Anisomycin selectively desensitizes signalling components involved in stress kinase activation and fos and jun induction. *Mol Cell Biol*. **18**:1844–54.

Hoffman DA, Sprengel R, Sakmann B (2002) Molecular dissection of hippocampal theta-burst pairing potentiation. *PNAS* **99**:7740–7745.

Huang YY and Kandel ER (1995) D1/D5 receptor agonists induce a protein synthesis-dependent late potentiation in the CA1 region of the hippocampus. *PNAS* **92**:2446–2450.

Huber KM, Kayser MS, Bear MF (2000) Role for rapid dendritic protein synthesis in hippocampal mGluR-dependent long-term depression. *Science* **288**:1254–1257.

Huganir RL and Nicoll RA (2013) AMPARs and synaptic plasticity: the last 25 years. *Neuron* **80**:704–717.

Kahn RS, Sommer IE, Murray RM, Meyer-Lindenberg A, Weinberger DR, Cannon TD, O'Donovan M, Correll CU, Kane JM, van Os J, Insel TR (2015) Schizophrenia. *Nat Rev Dis Primers*. **1**:15067.

Kebabian J and Calne D (1979) Multiple receptors for dopamine. *Nature* **277**:93–96.

Kyriakis JM, Banerjee P, Nikolakaki E, Dai T, Rubie EA, Ahmad MF, Avruch J, Woodgett JR (1994) The stress-activated protein kinase subfamily of c-Jun kinases. *Nature* **369**:156–160.

Matthies H, Becker A, Schröeder H, Kraus J, Höllt V, Krug M (1997) Dopamine D1-deficient mutant mice do not express the late phase of hippocampal long-term potentiation. *Neuroreport* **8**:3533–3535.

Mayr B and Montminy M (2001) Transcriptional regulation by the phosphorylation-dependent factor CREB. *Nat Rev Mol Cell Biol.* **2**:599–609.

Nobili A, Latagliata EC, Viscomi MT, Cavallucci V, Cutuli D, Giacovazzo G, Krashia P, Rizzo FR, Marino R, Federici M, De Bartolo P, Aversa D, Dell'Acqua MC, Cordella A, Sancandi M, Keller F, Petrosini L, Puglisi-Allegra S, Mercuri NB, Coccurello R, Berretta N, D'Amelio M (2017) Dopamine neuronal loss contributes to memory and reward dysfunction in a model of Alzheimer's disease. *Nat Commun*. **8**:14727.

O'Carroll CM, Martin SJ, Sandin J, Frenguelli B, Morris RG (2006) Dopaminergic modulation of the persistence of one-trial hippocampus-dependent memory. *Learn Mem*. **13**:760–769.

Otmakhova NA, and Lisman JE (1998) D1/D5 dopamine receptors inhibit depotentiation at CA1 synapses via cAMP-dependent mechanism. *J. Neurosci*. **18**:1270–1279.

Park P, Georgiou J, Sanderson TM, Ko KH, Kang H, Kim JI, Bradley CA, Bortolotto ZA, Zhuo M, Kaang BK, Collingridge GL (2021) PKA drives an increase in AMPA receptor unitary conductance during LTP in the hippocampus. *Nat Commun*. **12**:413.

Park P, Kang H, Sanderson TM, Bortolotto ZA, Georgiou J, Zhuo M, Kaang BK, Collingridge GL (2019) On the Role of Calcium-Permeable AMPARs in Long-Term Potentiation and Synaptic Tagging in the Rodent Hippocampus. *Front Synaptic Neurosci*. **11**:4.

Plant K, Pelkey KA, Bortolotto ZA, Morita D, Terashima A, McBain CJ, Collingridge GL, Isaac JT (2006) Transient incorporation of native GluR2-lacking AMPA receptors during hippocampal long-term potentiation. *Nat Neurosci*. **9**:602–604.

Poewe W, Seppi K, Tanner CM, Halliday GM, Brundin P, Volkmann J, Schrag AE, Lang AE (2017) Parkinson disease. *Nat Rev Dis Primers* **3**:17013.

Purkey AM, Dell'Acqua ML (2020) Phosphorylation-Dependent Regulation of Ca2+-Permeable AMPA Receptors During Hippocampal Synaptic Plasticity. *Front Synaptic Neurosci.* **12**:8.

Romberg C, Raffel J, Martin L, Sprengel R, Seeburg PH, Rawlins JN, Bannerman DM, Paulsen O (2009) Induction and expression of GluA1 (GluR-A)-independent LTP in the hippocampus. *Eur J Neurosci.* **29**:1141–1152.

Rossato JI, Bevilaqua LR, Izquierdo I, Medina JH, Cammarota M. (2009) Dopamine controls persistence of long-term memory storage. *Science* **325**:1017–1020.

Sassone-Corsi P (1995) Transcription factors responsive to cAMP. *Annu Rev Cell Dev Biol* **11**:355–377.

Sassone-Corsi P (2012) The cyclic AMP pathway. *Cold Spring Harb Perspect Biol* **4**:a011148.

Schmidt EK, Clavarino G, Ceppi M, Pierre P (2009) SUnSET, a nonradioactive method to monitor protein synthesis. *Nat Methods* **6**:275–277.

Shohamy D and Adcock RA (2010). Dopamine and adaptive memory. *Trends Cogn Sci.* **14**:464–72.

Smith WB, Starck SR, Roberts RW, Schuman EM (2005). Dopaminergic stimulation of local protein synthesis enhances surface expression of GluR1 and synaptic transmission in hippocampal neurons. *Neuron* **45**:765–79.

Stockwell I, Watson JF, Greger IH (2024) Tuning synaptic strength by regulation of AMPA glutamate receptor localization. *Bioessays*. **1**:e2400006.

Takeuchi T, Duszkiewicz AJ, Sonneborn A, Spooner PA, Yamasaki M, Watanabe M, Smith CC, Fernández G, Deisseroth K, Greene RW, Morris RG (2016) Locus coeruleus and dopaminergic consolidation of everyday memory. *Nature* **537**:357–362.

Wang H, Pineda VV, Chan GC, Wong ST, Muglia LJ, Storm DR (2003) Type 8 adenylyl cyclase is targeted to excitatory synapses and required for mossy fiber long-term potentiation*. J Neurosci*. **23**:9710–9718.

Wenthold RJ, Petralia RS, Blahos J II, Niedzielski AS (1996) Evidence for multiple AMPA receptor complexes in hippocampal CA1/CA2 neurons. *J Neurosci.* **16**:1982-9.

Zhang D, Ivica J, Krieger JM, Ho H, Yamashita K, Stockwell I, Baradaran R, Cais O, Greger IH (2023) Structural mobility tunes signalling of the GluA1 AMPA glutamate receptor. *Nature* **621**: 877–882.

Zamanillo D, Sprengel R, Hvalby O, Jensen V, Burnashev N, Rozov A, Kaiser KM, Köster HJ, Borchardt T, Worley P, Lübke J, Frotscher M, Kelly PH, Sommer B, Andersen P, Seeburg PH, Sakmann B (1999). Importance of AMPA receptors for hippocampal synaptic plasticity but not for spatial learning. *Science* **284**:1805–1811.

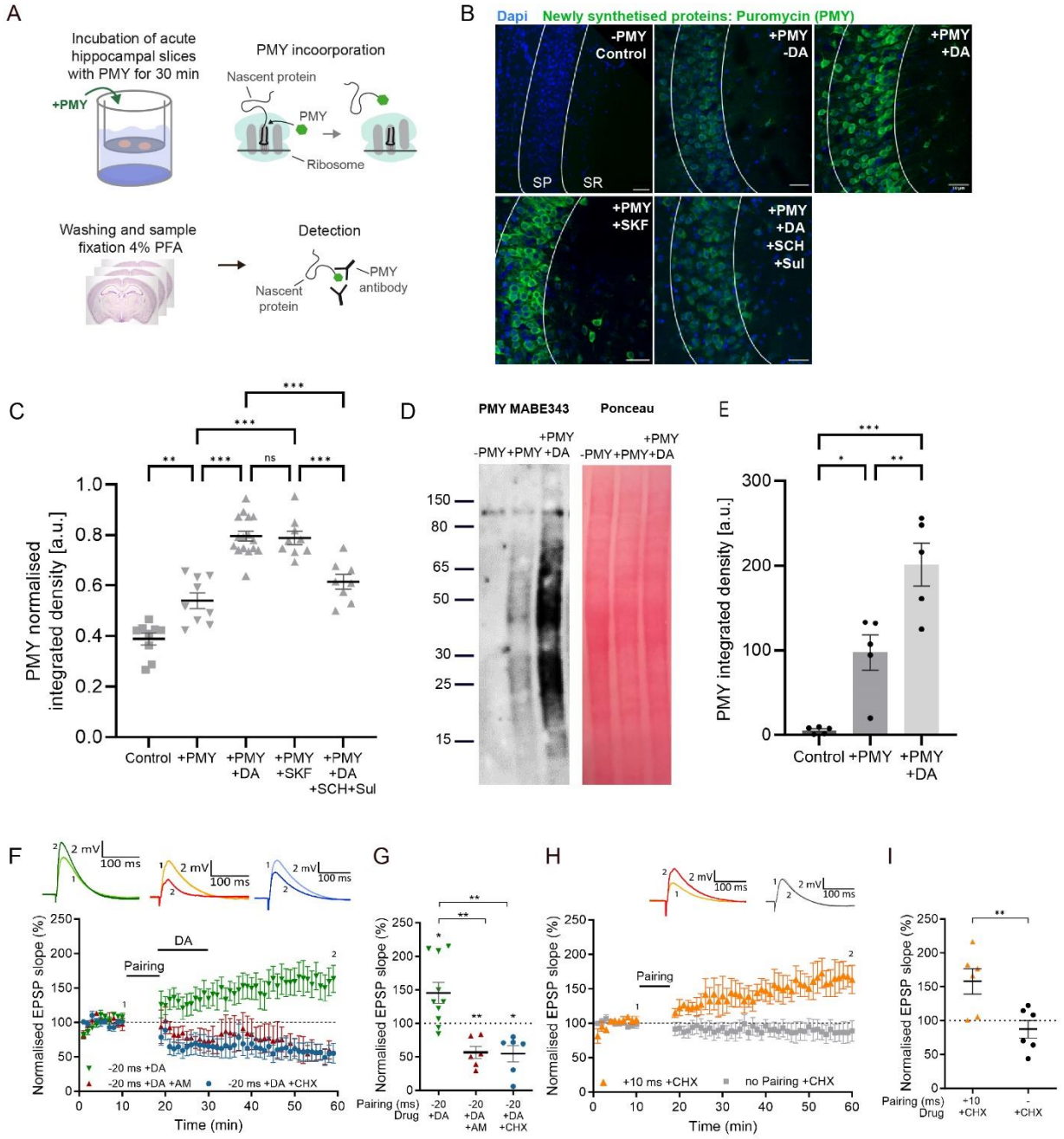


**Figure 1**. Dopamine increases protein synthesis in CA1, required for DA-LTP, but not for conventional t-LTP. (**A**), Experimental workflow for protein synthesis labelling in acute hippocampal slices using SUnSET. PMY = puromycin. (**B**), Representative images of the CA1 region of the hippocampus (SP: stratum pyramidale, SR: stratum radiatum) of puromycin-labelled proteins (green) and Dapi (blue) in the following conditions: negative control (no PMY), PMY alone, PMY + dopamine (DA), PMY + SKF38393 (SKF), and PMY +DA + SCH23390 (SCH) + Sulpiride (Sul). The slices show an increase in protein synthesis after DA or SKF38393 application, which is blocked by DA receptor antagonists SCH23390 and Sulpiride. Scale bar, 30 µm. (**C**), Summary of results. One-way ANOVA followed by Tukey's HSD test, **, $p < 0.01$; ***, $p < 0.001$;

ns, not significant. (**D**), Representative western blot of newly synthesised proteins detected by PMY Mabe343 antibody shows no signal in negative control (-PMY), and increased PMY signal in the presence of dopamine (+DA). Ponceau stain confirms equal loading of total protein. (**E**), Summary of results. One-way ANOVA followed by Tukey's HSD test, *, $p < 0.05$; **, $p < 0.01$; ***, $p < 0.001$. (**F**), Dopamine application (DA) after a post-before-pre pairing protocol (Pairing, $\Delta t = -20$ ms) leads to synaptic potentiation (green trace), which is blocked by postsynaptically applied anisomycin (AM) (red trace) or cycloheximide (CHX) (blue trace). (**G**), Summary of results. *t*-test, **, $p < 0.01$. (**H**), Intact conventional t-LTP ($\Delta t = +10$ ms, orange trace) in the presence of cycloheximide (CHX). (**I**), Summary of results. *t*-test, **, $p < 0.01$. Traces show an EPSP before (1) and 40 minutes after (2) pairing. Plots show averages of normalised EPSP slopes ± SEM.

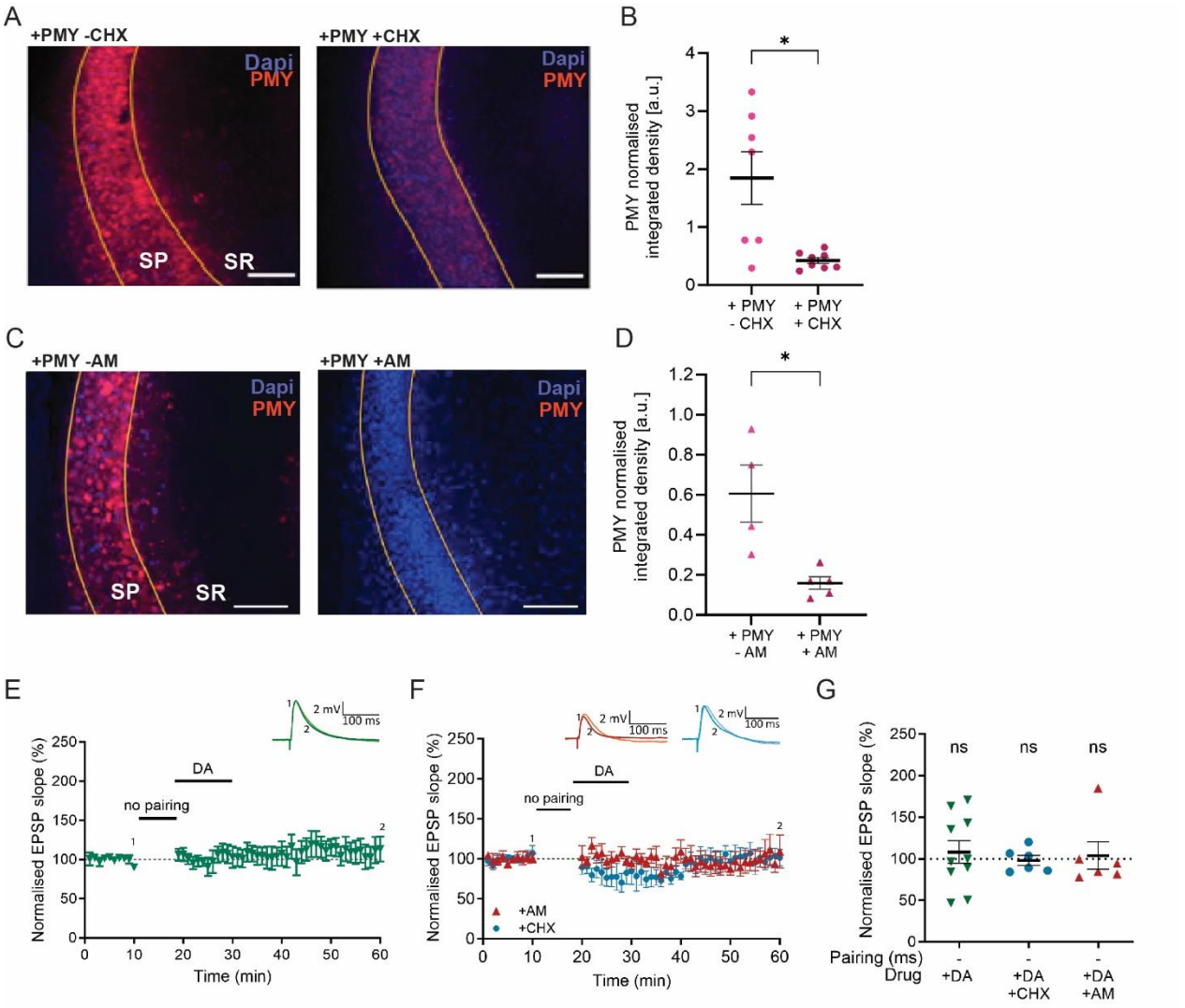


**Figure 1S**. SUnSET assay is specific to protein synthesis and protein synthesis inhibitors do not affect baseline synaptic transmission within 60 minutes of recording. (**A, C**), Representative images of the CA1 region of the hippocampus (SP: stratum pyramidale, SR: stratum radiatum) of puromycin-labelled proteins (PMY, red) and Dapi (blue). Puromycin incorporation is significantly reduced in the presence of the protein synthesis inhibitors (**A**) cycloheximide (CHX) or (**C**) anisomycin (AM). Scale bar, 80 µm (**B**, **D**), Summary of results. t-test, *, $p < 0.05$ (**E**), Dopamine application alone, without prior pairing, does not affect synaptic weights in control pathway (green trace). (**F**), Postsynaptically applied anisomycin (AM) (red trace) or cycloheximide (CHX) (blue trace) does not affect synaptic weights throughout recording. Traces show an EPSP before (1) and 40 minutes after (2) pairing. Plots show averages of normalised EPSP slopes ± SEM. (G), Summary of results. *t*-test, ns, not significant.

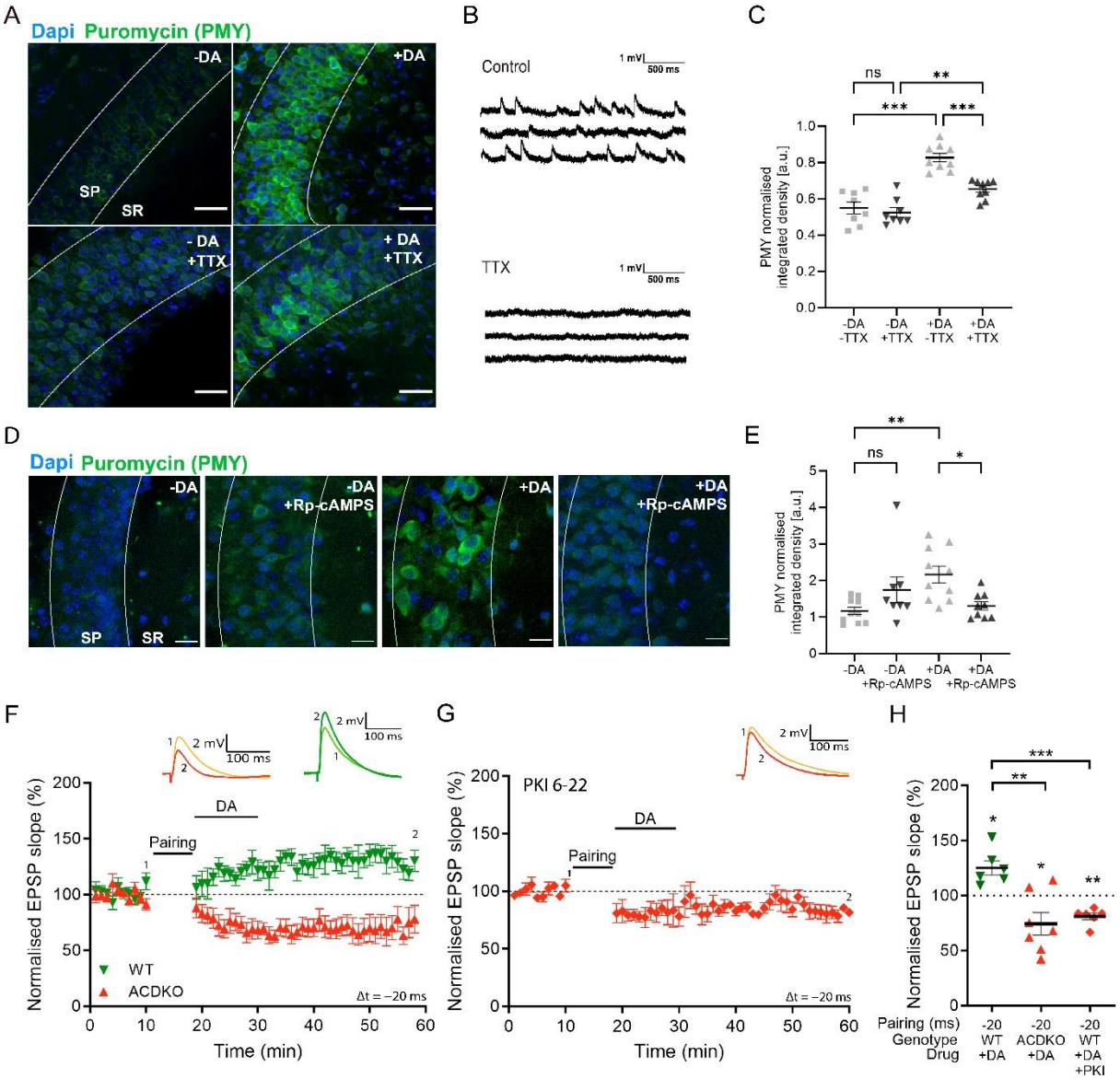


**Figure 2.** Dopamine and neuronal activity mediate increase in protein synthesis via AC1/8 and PKA enabling DA-LTP. (**A**), Representative images of the CA1 region (SR: stratum oriens, SP: stratum pyramidale) of the hippocampus of puromycin-labelled proteins in the following conditions: PMY alone (-DA), PMY+dopamine (+DA), PMY+TTX (-DA+TTX), PMY+dopamine+TTX (+DA+TTX). Images show that the dopamine-induced increase in protein synthesis is reduced in the presence of TTX. Scale bar, 30 µm. (**B**), TTX abolishes spontaneous activity shown in traces of whole-cell patch clamp recording. (**C**), Summary of results. One-way ANOVA followed by Tukey's HSD test, **, $p < 0.01$; ***, $p < 0.001$; ns, not significant. (**D**), Representative images of the CA1 region (SR: stratum oriens, SP: stratum pyramidale) of the hippocampus of puromycin-labelled proteins in the following conditions: PMY alone (-DA), PMY+Rp-cAMPS (-DA+Rp-cAMPS, PMY+dopamine (+DA), and PMY+dopamine+Rp-cAMPS (+DA+Rp-cAMPS). Images show that the dopamine-induced increase in protein synthesis is prevented by Rp-cAMPS. (**E**), Summary

of results. One-way ANOVA followed by Tukey's HSD test, *, $p < 0.05$; **, $p < 0.01$; ns, not significant. (**F**), Dopamine application (DA) after a post-before-pre pairing protocol (Pairing, $\Delta t = -20$ ms) leads to synaptic potentiation in WT (green trace), but not in AC DKO mice (red trace). (**G**), Postsynaptically applied PKA inhibitor PKI6-22 blocks DA-LTP (red trace), leaving synaptic depression instead. (**H**), Summary of results. One-way ANOVA followed by Tukey's HSD test, **, $p < 0.01$; ***, $p < 0.001$. Traces show an EPSP before (1) and 40 minutes after (2) pairing. Plots show averages of normalised EPSP slopes ± SEM.

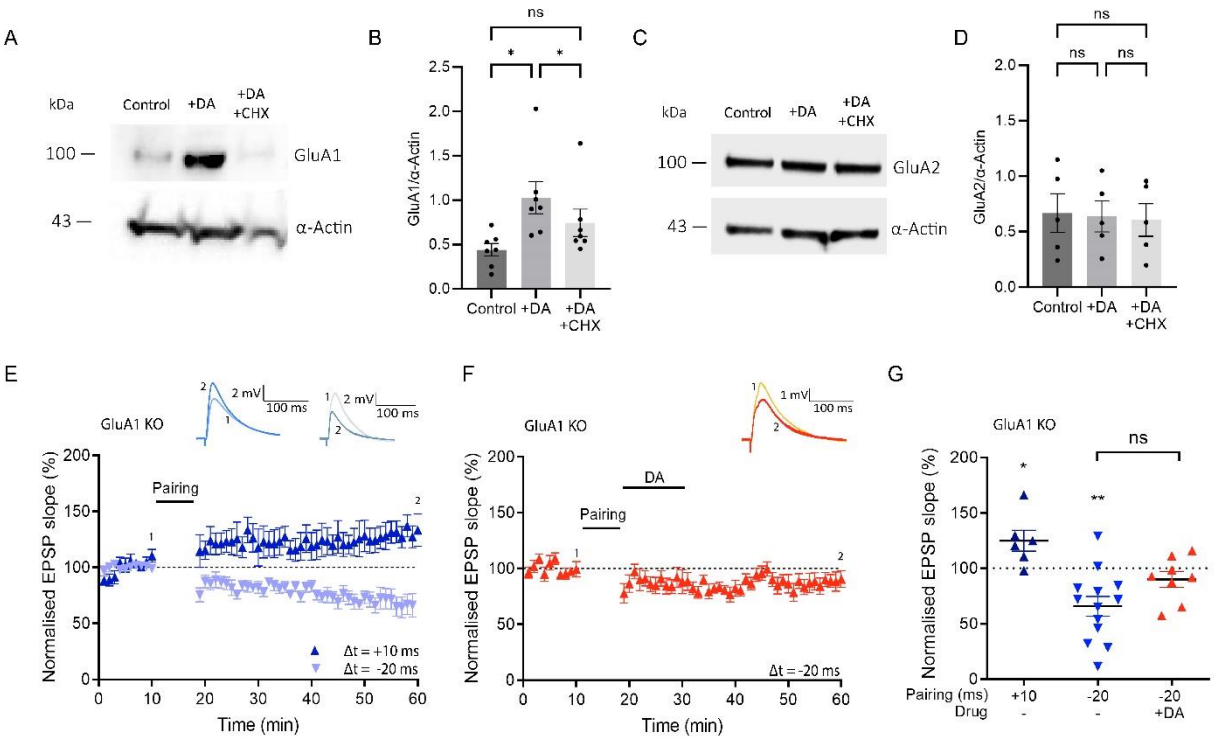


**Figure 3.** Dopamine increases GluA1 in a protein synthesis-dependent manner, which is required for DA-LTP. (**A**), Western blot images from tissue homogenates of the hippocampal CA1 region shows increase of GluA1 upon dopamine application (+DA), which is abolished in the presence of cycloheximide (+DA +CHX). α-Actin was used as loading control. (**B**) Summary of results. One-way ANOVA followed by Tukey's HSD test, *, $p < 0.05$; ns, not significant. (**C**) Western blot shows unchanged GluA2 following dopamine application (DA) and no change with cycloheximide (+DA +CHX). (**D**), Summary of results. One-way ANOVA followed by Tukey's HSD test, ns, not significant. (**E**), A t-LTP pairing protocol (Δt = +10 ms) induces potentiation (dark blue trace), and a t-LTD protocol (Δt = –20 ms) induces depression (light blue trace) in GluA1 KO mice, (**F**) No DA-LTP in GluA1 KO mice. (**G**), Summary of results. All traces show an EPSP before (1) and 40 minutes after (2) pairing. Plots show averages of normalised EPSP slopes ± SEM. *t*-test, *, $p < 0.05$; **, $p < 0.01$; ns, not significant.

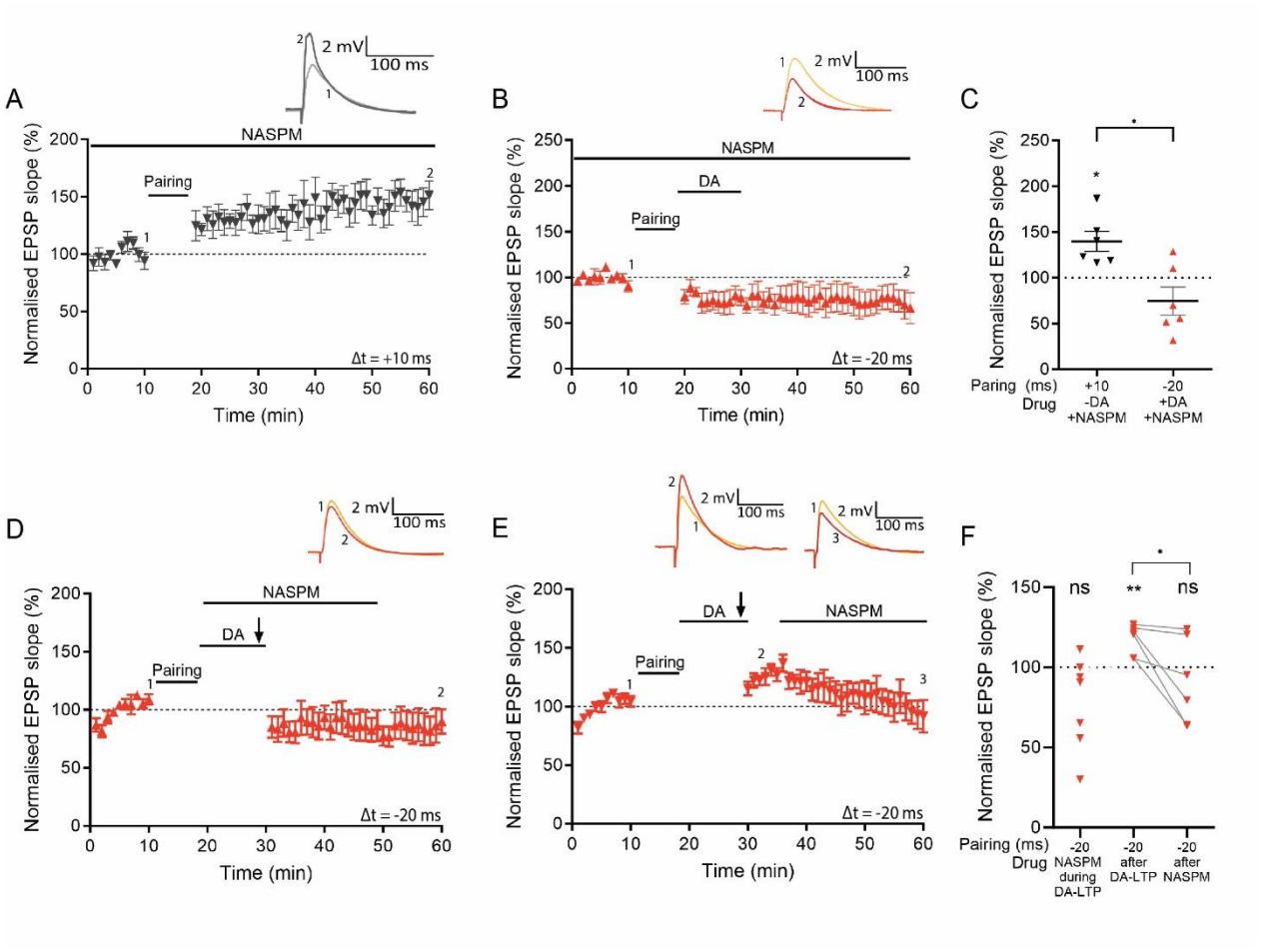


**Figure 4**. CP-AMPARs are required for DA-LTP but not for conventional t-LTP. (**A**), A t-LTP pairing protocol (Δt = +10 ms) induces synaptic potentiation in the presence of extracellularly applied NASPM. (**B**), NASPM blocks DA-LTP. (**C**), Summary of results. *t*-test, *, $p < 0.05$. (**D**), Burst-induced DA-LTP is blocked by NASPM. (**E**) Burst-induced DA-LTP potentiation decreases when NASPM is applied 7 minutes afterwards. (**F**), Summary of results. *t*-test, *, $p < 0.05$; **, $p < 0.01$; ns, not significant. Traces in (**A, B** and **D**) show an EPSP before (1) and 40 minutes after pairing (2). Traces in (**E**) show an EPSP before (1), 5 minutes after DA and burst stimulation (2), and 40 minutes after pairing (3). Plots show averages of normalised EPSP slopes ± SEM.

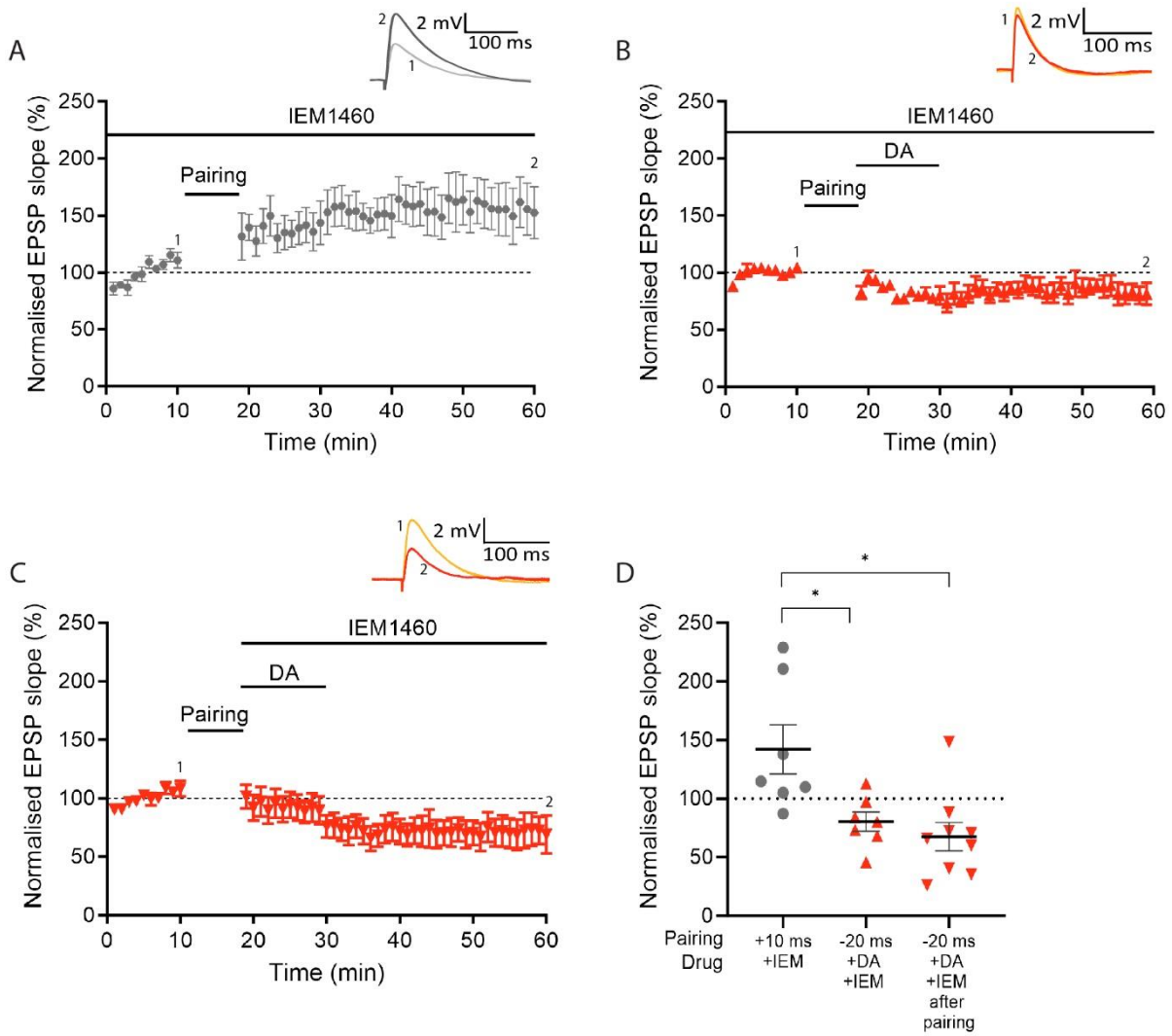


**Figure 4S**. CP-AMPARs blocker IEM-1460 confirms that CP-AMPARs are required for DA-LTP but not for conventional t-LTP. (**A**), A t-LTP pairing protocol (Δt = +10 ms) induces synaptic potentiation in the presence of extracellularly applied IEM-1460. (**B, C**), IEM-1460 blocks DA-LTP, whether applied throughout (**B**) or after the pairing protocol (**C**). (**D**), Summary of results. *t*-test, *, $p < 0.05$. Traces show an EPSP before (1) and 40 minutes after pairing (2). Plots show averages of normalised EPSP slopes ± SEM.